Optimal optical trap for bacterial viability

Utkur Mirsaidov,[1] Winston Timp,[2,*] Kaethe Timp,[1] Mustafa Mir,[1] Paul Matsudaira,[2] and Gregory Timp[1]

[1]*Beckman Institute, University of Illinois, Urbana, Illinois 61801, USA*

[2]*Whitehead Institute, M.I.T., Cambridge, Massachusetts 02142, USA*

Optical trapping is a powerful tool for the micromanipulation of living cells—especially bacteria—but photodamage induced by the laser beam can adversely affect viability. We have explored optical trapping conditions in the near infrared (840–930 nm) that preserve the viability of *E. coli*, as measured by gene expression of green fluorescent protein. We have found that time-sharing the optical traps, i.e., dwelling only 10 μs–1 ms on the cell, improves viability relative to continuous wave (CW) exposure for the same exposure time. We have also observed that similar to CW traps the photodamage in a time-shared trap depends weakly on wavelength, but linearly on peak power, implying an effect induced by single photon absorption. Taken altogether, integrating the exposure time and peak power, the data indicate that there is a lethal *energy* dose of about 5 J for *E. coli*. Thus a single parameter—the energy—can be used to describe the limitation on viability.

PACS number(s): 87.80.Cc, 87.85.dh, 87.80.Fe

INTRODUCTION

Optical micromanipulation in biological systems has undergone a revolution [1]. Twenty years ago, pioneering work by Ashkin demonstrated that optical tweezers—produced by focusing a single TEM$_{00}$ laser beam of wavelength λ to the diffraction limit with a high numerical aperture (NA) microscope objective—could displace and levitate bacteria, and even manipulate organelles within living cells [2–6]. Although the trapping force is weak (~1 nN), cells have a miniscule mass (a bacterium weighs about 10 fN), allowing optical tweezers to be effective for micromanipulation of living tissue.

Recently, it has been shown that two or more optical traps arrayed together can be especially useful for manipulating living cells, and several beam-steering strategies have already been employed to produce them [7–14]. For example, using these strategies we recently demonstrated the ability to assemble three-dimensional, heterotypic microarrays of living cells that resemble tissue [7]. Multiple traps can be created by time-sharing the beam between different positions in the array, scanning rapidly from one trap position to the next, faster than the bacteria move away, then dwelling at the desired position in the array just long enough to form an optical trap and fix the location of the cell. As long as the bacteria move less during the dark time than the thermal fluctuation in an optical trap during the bright time, it is actually more advantageous to use time-shared beams to trap because the deeper optical potential provides better confinement for the same time-averaged power. The only limitation is that the restoring force due to the potential must have enough bright time to bring the bacterium back to the trap focus from the displacement, which occurred in the dark.

Minimizing the photodamage in the trap beam is vital for manipulating living cells [15–21]. Neuman *et al.* [21] have reported wavelength-specific adverse effects of optical trap-

ping on bacterial viability with continuous wave (CW) exposure. They showed that a change in the wavelength from 930 nm (most damaging) to 830 nm (least damaging) affects the lethal dose for *E. coli* by about a factor of 5. They measured viability by monitoring the rotation rate of cells tethered to a glass cover slip by means of a single flagellum, as the rotation rate is proportional to the transmembrane potential. Assays like this for proton pumping, respiration, or uptake of substrates are used to measure metabolic activity. However, these assays may not discriminate effectively between live and dead cells (especially for bacteria) since the activity of the cells may be below the threshold for detection. Assays that detect the pH gradient [22] across the cell membrane suffer the same limitation. On the other hand, viability assays using LIVE/DEAD stains to test membrane integrity have been found to correspond to about 90% clonal efficiency with limited exposure to the trapping beam [23].

We hypothesize that minimizing the total energy delivered to the cell by the laser beam in an optical trap will preserve viability from single photon damage. To test this hypothesis, we used gene expression of green fluorescent protein (GFP) in *E. coli* exposed to time-multiplexed and CW optical traps as a test for viability. Gene expression has been used in prior work to measure the stress response caused by optical tweezers in a eukaryote, *C. elegans* [24]. Since gene manipulation and regulation of gene expression is easily accomplished in prokaryotes, we incorporated a reporter gene into *E. coli*, encoding GFP in response to an inducer to monitor cell metabolism in real time. To track the activity of individuals for up to 12 h after exposure, we assembled the cells using optical traps into two-dimensional (2D) 5×5 microarrays, held them in the array for a prescribed exposure time, and then fixed the position of the cells in a hydrogel scaffold made from a photopolymerized polyethylene glycol diacrylate (PEGDA) and terminated exposure to the trapping beam. PEGDA hydrogels are especially effective as a scaffold because they have demonstrated biocompatibility: i.e., bacteria and eukaryotes can remain viable for weeks encapsulated in a hydrogel environment [25,26]. So, for each bacterium that we manipulate into an array in hydrogel, we are actually assessing not only photodamage, but also cytotoxicity and

---

*Contact person for information regarding genetics, hydrogel, and data analysis.

cytocompatibility of the photoinitiator [27], and biocompatibility in the hydrogel.

We have identified the optical trapping conditions in the near infrared (IR) band from 840 to 930 nm required to preserve viability in *E. coli*, as measured by gene expression of GFP. In what follows, we show that time-sharing the optical traps increases the number of *E. coli* expressing GFP relative to the same exposure time to a CW beam with the same peak power. We find a linear dependence of viability on peak power, which implies that photodamage is dominated by single photon absorption. In stark contrast to prior work by Neuman *et al.* on *E. coli*, we find a wavelength dependence that shows the most damage at $\lambda = 870$ nm and the least at 900 nm, although the variation in viability is only about 20% across the entire 840–930 nm band. When it is related to the time-averaged power, the viability observed for a time-shared optical trap follows the same wavelength and power dependence observed for a CW trap. Generally, for the same duration exposure, the photodamage is related to the time-averaged power, not the peak power, while for the same time-averaged power, the photodamage increases linearly with the exposure time. Taken altogether, integrating the exposure time and power, the data indicate that there is a single parameter—the energy—that affects viability.

MATERIALS AND METHODS

As illustrated in Fig. 1, we formed microarrays of bacteria using optical tweezers produced from a CW Ti:Sap laser beam and a Zeiss Achroplan $100\times$ oil immersion objective (1.25NA) held in an inverted optical microscope (Zeiss Axiovert 200M). We used two different methods to produce multiple traps that employed *either* acousto-optic deflectors (AODs) to create time-shared traps, or a spatial light modulator (SLM) to produce CW, holographic optical traps (HOT). To form multiple, time-multiplexed optical traps we used the AODs (from AA-Optoelectronic) with the SLM acting like a mirror. In this configuration, the CW Ti:Sap beam is deflected transverse to the direction of propagation using two orthogonally mounted AODs to give independent control of the x and y positions of a trap. The beam is time-shared between different positions in the 2D array, i.e., it is scanned rapidly from one trap position to the next, dwelling at the desired position in the array just long enough to form an optical trap and fix the location of the cell [12]. Typically, the laser beam was deflected between 25 trap positions in a 5 $\times$ 5 array at a 4 kHz rate with a dwell time of the trap over a particular position of 10 μs. The inset to Fig. 1 shows a microarray of bacteria produced under these conditions.

We formed similar arrays by generating CW, HOTs with the SLM (Boulder Nonlinear Systems) instead of using time-shared optical traps. The SLM is an optically addressed nematic liquid crystal device configured to act as a phase hologram with 256 gray levels. It has near-VGA resolution without sharp spatial pixelation, which gives first-order diffraction efficiencies larger than 90%. The SLM was used to introduce phase shifts to implement a 2D diffraction grating. To determine the phase distribution in the SLM plane required to produce the desired intensity distribution in the trapping plane, we used the Gerchberg-Saxton algorithm, described in detail elsewhere [28].

Relay lenses were used to image the beam emerging from the AOD or SLM onto the back aperture of the objective [29]. Typically, the cells were trapped about 5 μm above the surface of the coverslip to minimize spherical aberrations from the media. We measured the power incident on the back aperture of the objective for each wavelength and then corrected for the transmission through the objective using transmission curves provided by Zeiss [30]. The transmission over the wavelength range $840 \le \lambda \le 930$ nm was approximately 73%.

We chose to assess the viability of the *E. coli* strain DH5α (Invitrogen #18258-012). The *E. coli* was transformed with a plasmid coded GFP-M1 and selected by ampicillin resistance. The GFP-M1 plasmid, shown in Fig. 2(a), uses the pBR322 origin of replication providing 15–20 plasmid copies per cell. It contains a gene encoding GFP under the control of the *lac* operon. We induced the transformed cells using IPTG (Isopropyl β-D-thiogalactopyranoside). IPTG binds to the repressor protein and allows transcription, reported through the production of green fluorescent protein. Thus a fluorescent signal from the cell indicates gene expression and an active cell metabolism.

The threshold IPTG concentration for induction in GFP-M1 transformed bacteria was determined by measuring fluorescence of single bacteria taken from a log-phase culture. ($OD_{633} = 0.33 \pm 0.08$ at $T = 25$ °C.) The transformed bacteria were grown from the culture in M9-Glycerol minimal media consisting of 0.2% (v/v) glycerol, 42 mM Na_2HPO_4; 22 mM KH_2PO_4; 20 mM NH_4Cl; 10 mM NaCl; 1 mM $MgSO_4$; 100 μM $CaCl_2$; 200 μM thiamine; and 0.2% (w/v) casamino acids with ampicillin (100 μg/ml) (Sigma Aldrich A5354) as a selection marker. Fluorescence data were collected by using a Cytomation MoFlo MLS flow cytometer and cell sorter at a low flow rate, exciting the GFP with a 488 nm argon laser and detecting fluorescence using a 515–545 nm emission filter. Green fluorescent microspheres (Invitrogen) were used to calibrate the flow of cytometer; determining fluorescence, sensitivity, and size measurements. For each concentration of IPTG, a fluorescent measurement of gene expression was obtained from one culture. Two measurements were made for each culture: ~23 000 induced cells with ~23 000 uninduced cells used as a control. The introduction of a scattering filter normalizes the cellular size and morphology variability, providing a better basis for comparison. Figure 2(b) shows the number of active (expressing GFP) and inactive (not expressing GFP) bacteria as a function of IPTG concentration. The threshold for inactive bacteria was set by the autofluorescence associated with uninduced bacteria. The threshold concentration, defined as the IPTG concentration at which expression is 50% of maximum, was determined to be 24 μM of IPTG at 25 °C. At 10 mM, 81% of the bacteria are expressing GFP.

While optical trapping can be used to create vast networks of cells resembling tissue, the trapping beam must be held on the cells to maintain the array. To follow the GFP production in individuals for up to 12 h, we permanently fixed the position of the cells in the array with a photopolymerizable PEGDA hydrogel [7,31–34] and then terminated exposure to
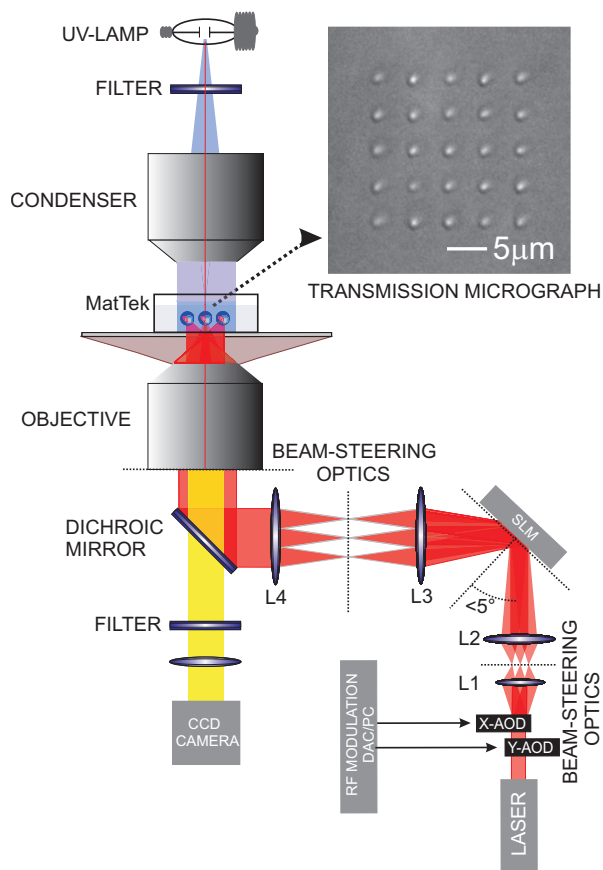
FIG. 1. (Color) Schematic diagram of a time-shared and holographic optical trapping apparatus. Two-dimensional (2D) trap arrays are formed using a Zeiss Achroplan high NA objective (100× /1.25 NA) commercial Axiovert 200M optical microscope in conjunction with either one of two diffractive elements: i.e., two acousto-optic deflectors, or a spatial light modulator. The same microscope that is used to produce the cell traps is also used for viewing (via the yellow beam) and photopolymerizing the PEGDA hydrogel (via the blue beam). The inset in the upper right shows an example of a 2D 5×5 array of *E. coli* formed using this apparatus and subsequently embedded in hydrogel. The distances are AODs: L1=400 mm; L1 L2=800 mm; L2 entrance pupil=400 mm; L3 L4=800 mm; and L4 OEA=420 mm, where the focal lengths for L1, L2, L3, L4 are 400 mm.

the trapping beam. We formed the hydrogel from a prepolymer mix consisting of PEGDA (MW=3400 Da) dissolved in M9 minimal media without the thiamine and casamino acids to yield a 5% (w/v) final concentration. 1 mL samples of bacteria grown in M9 overnight at 25 °C were centrifuged three times for 5 min at 800 g. Between each spin cycle the supernatant was aspirated, and the bacterial pellet resuspended in 1 mL of M9 Glycerol media. Finally, a prepolymer mixture comprised of 3400 Da MW PEGDA (Nektar Therapeutics) dissolved at 5% (w/v) in M9-Glycerol along with photoinitiator, 2-hydroxy-2-methyl-priophenone at a concentration of 0.2% (v/v) was vigorously vortexed for 1 min, and then combined with the cell suspension to create the desired concentration of PEGDA immediately before trapping. The cell and PEGDA suspension was 100 μL pipetted onto MatTek® dishes and placed on the microscope.
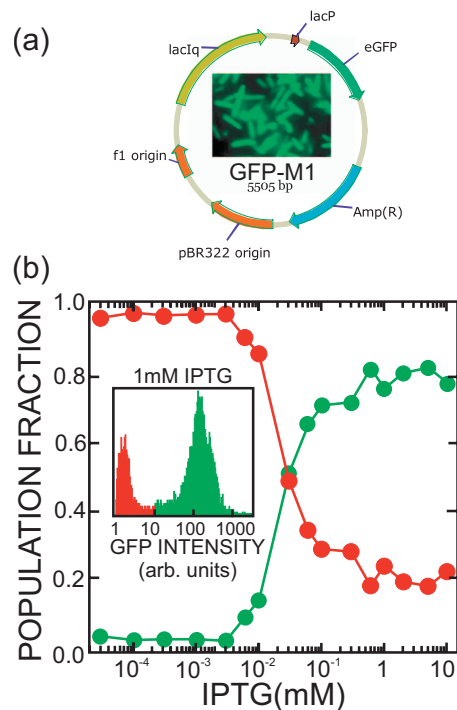

FIG. 2. (Color) (a) The receiver plasmid, GFP-M1, is the focus of this work. It combines the *lac* operon with green fluorescent protein (GFP). Induction by IPTG initiates GFP production. The resulting fluorescence is used to indicate an active cell metabolism. (b) Threshold for induction of M1's by IPTG at 25 °C. Bacteria count measured using laser cytometry for 23 000 *E. coli* cultured at 25 °C. A typical distribution as a function of the fluorescent intensity obtained for 1 mM IPTG is shown in the inset. The active cell count indicated by green fluorescence is shown in green, and the inactive is shown in red. The IPTG threshold estimated from a fit to the data is 24 μM. Only about 80% of the cells are active even at high IPTG concentration.

A microarray was assembled using optical tweezers to manipulate the bacteria in a MatTek® dish. Typically, it takes less than 2 min to form an array, but to be consistent and make contact with earlier work [21], each bacterium in the array was held in the trap for 7–8 min prior to photopolymerizing the hydrogel. The prepolymer solution was then exposed to light from a filtered 100 W Hg lamp to form the gel, while at the same time exposure to the trapping beam was terminated. A beam of UV light in the band λ =360±20 nm with a waist of 2.1 mm and a total power of 4–5 mW was stopped to a 600 μm diameter spot that exposed the hydrogel for 1–6 s. The exposure was minimized to ensure clonal efficiency and avoid cell damage. We found that *E. coli* proliferation was not adversely affected for UVA exposures less than 60 s. However, it has been reported that cell death based on nonthermal, photochemical reactions like photo-oxidation can occur with 1 J/cm^2 to UVA (320–400 nm) for an interval of less than 1 min with the λ =365 nm line of a 100 W xenon arc lamp through a 0.55 NA condenser [35]. The encapsulated array was then washed with M9 media to remove residual cells and prepolymer. Subsequently, the microarrays in hydrogel were placed in a
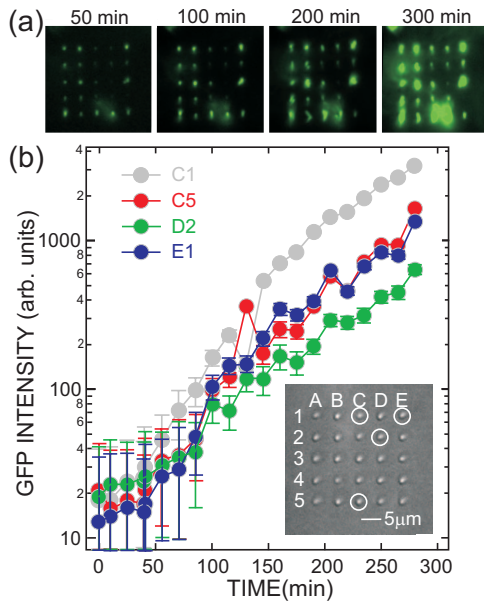
FIG. 3. (Color) Genetically identical cells express GFP gene differently due to the stochastic nature of biochemical processes. (a) Time evolution of green fluorescence in a 5×5 microarray of M1 bacteria following the induction using 10 mM IPTG at $t=0$. The bacterial array was assembled using time-shared optical traps formed using a beam with $P=140$ mW at $\lambda=900$ nm. The array was held for about 8 min prior to gelling. We can follow the development of the fluorescence associated with each cell in the array as a function of time. (b) A summary of the time development of the fluorescence measured on five cells in the array. The fluorescence usually saturates after about 5 h.

M9+ampicillin solution containing 10 mM of IPTG, which is more than enough to saturate the promoter activity at 25 °C.

We then measured the time dependence of the fluorescence, extracting the intensity from the time-lapse images using MATLAB (V7.2, MathWorks) along with the Image Processing Toolbox (V5.2, MathWorks). These fluorescence images, obtained using a 12-bit charge-coupled device camera (Hamamtsu ORCA-ER) indicate that GFP is being produced in the trapped cells after induction by IPTG. The images were recorded as 16-bit grayscale TIFFs, and subsequently read into two-dimensional numerical arrays containing the intensity values of each pixel in the image. The images were manually cropped around the cell array to facilitate automatic cell detection. The cropped images were filtered using a Gaussian bandpass filter to eliminate the low frequency background and high frequency pixelation noise. To detect the location of the cells expressing fluorescence, a 90% threshold value was used to mask the image. A watershed algorithm [36] was then used to separate the fluorescent pixel regions. The coordinates associated with the centers of each of these regions were recorded yielding the individual cell centers. Finally, the 90th percentile of the unfiltered intensity values of these regions was recorded and plotted. The corresponding fluorescence of selected bacteria is summarized in Fig. 3(b). Figure 3(b) reveals a distribution of response times associated to individuals in the cell array—information like this is usually obscured in bulk measurements of the fluorescence that cannot monitor the same cell at different times.
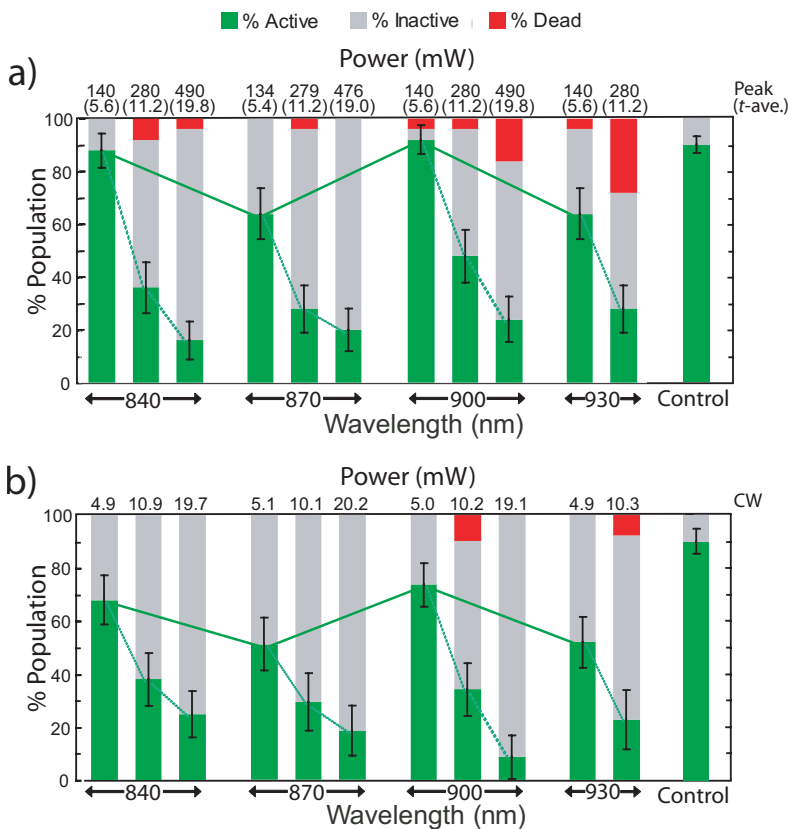

FIG. 4. (Color) Viability as a function of near IR wavelength, power for time-shared and static optical traps. (a) 5×5 2D arrays of *E. coli* bacteria incorporating the plasmid GFP-M1 are assembled using a time-shared optical trap with the specified wavelength and power. In each case the cells in the microarray are held for about 8 min prior to gelling. The peak power is indicated along with the corresponding time-averaged power in parentheses. The bar graph represents viable, active bacteria (green), inactive bacteria (gray), and dead bacteria (red) for each wavelength and power. Viability decreases nearly linearly with increasing power, and peaks at $\lambda=840$ and 900 nm. (b) Similar to (a) but now using a CW beam to form the 5×5 2D arrays of *E. coli*. The static CW in optical traps ranges from about 5 to 20 mW at the specified wavelength. Again, in each case the cells in the microarray are held for about 8 min prior to gelling. The CW viability tracks that found for the time-shared trap at about the same time-averaged power. The right side of the corner shows control bacteria, untrapped but encapsulated in the hydrogel spot.

RESULTS AND DISCUSSION

We are motivated to determine conditions suitable for optically trapping *E. coli* without adversely affecting viability. To acquire statistical data about the viability of a cell population, we tracked the time development of the green fluorescence of individual cells in 5×5 arrays that had been fixed in hydrogel scaffolds. The change in fluorescence with time indicates a viable cell with an active metabolism. So we monitored the time dependence of the fluorescence, extracting the intensity from the time-lapse images. A time-lapsed fluorescence image of a typical array formed using $P = 140$ mW at $\lambda = 900$ nm is shown in Fig. 3(a). The expression of GFP is an unequivocal measure of the cell metabolism after being subjected to the trap beam. In this case, 23 of the cells in the array (92%) expressed GFP. In contrast, GFP expression in M1 bacteria used as a control, which had been encapsulated in PEGDA but not exposed to the trapping beam, was $90 \pm 3\%$. Approximately 5 h after induction, the fluorescence saturates the camera. At that time, we used 1 μg/ml propidium iodide (Invitrogen: P3566) to test membrane integrity and subsequently report the red fluorescent cells as dead. It was apparent that most of the cells shown in Fig. 3 remained viable despite encapsulation in hydrogel because they have proliferated after 12 h. Figure 3(b) clearly illustrates the different gene expression level of individual bacteria rising from stochastic variation between cells [also evident from the expression levels shown in the inset of Fig. 2(b)].

To study the wavelength and power dependence of the lethal dose of IR radiation, we assembled 5×5 microarrays of the *E. coli* bacteria using optical traps at wavelengths $\lambda = 840, 870, 900,$ and 930 nm and with time-averaged optical power ranging from about 5 to 20 mW (after the objective) using a dwell time of 10 μs and a duty cycle of 1:25. Figure 4(a) represents the bacteria score corresponding to the cells in a 5×5 microarray 5 h after exposure to a time-shared trapping beam. (The number of cells for each data point in the histogram is given in Table S1 in the supplementary materials [37].) The number of active cells, evident from the expression of GFP, is represented by green; the number of inactive bacteria with no gene expression, but an intact membrane, is represented by gray; and the number of bacteria lacking membrane integrity is shown in red. The power in the beam is ~140, 280, or 490 mW with a duty cycle of 1:25 corresponding to time-averaged power levels of 5.6, 11.4, and 19.6 mW, respectively.

With increasing power in the beam, we find a monotonic decrease in the viability measured by the green bacteria score—notice that the number of active cells drops by about a factor of 2 when the power doubles, regardless of the wavelength. A simple model for the photodamage relates the sensitivity S to the time-averaged power P delivered to the specimen: $S(P) = A + BP^n$, where A is the control sensitivity and B is the wavelength-dependent sensitivity [21]. For a single photon process this relationship is linear ($n = 1$). $S(P)$ is defined as the reciprocal of the glowing (gene expression) to total number of the bacteria in the array. We also assume that the control sensitivity vanishes since presumably photodamage by the laser is the only factor contributing to loss of viability. As shown in the supplementary materials, fitting the data yields an index n for time-shared traps [37]. For the time-shared traps we find $n = 1.34 \pm 0.04$ at 840 nm; $n = 0.93 \pm 0.14$ at 870 nm; and $n = 1.1 \pm 0.1$ at 900 nm. Since the exponent for time-shared traps is about $n = 1$ this suggests a linear relationship indicating that the photodamage is predominately due to a one-photon process induced via absorption. The number of lysed cells indicated by red also seems to increase with increasing power at some wavelengths, but not others.

Figure 4(a) also scores the sensitivity of *E. coli* to the wavelength of the optical trap. We find that the spectrum for photodamage exhibits only weak minima at $\lambda = 870$ and 930 nm with ~20% degradation in activity between the peak at 900 nm (92%) to the minimum at 870 nm (65%), while the M1 bacteria used as a control showed about 90% viability. (Corresponding to Fig. 4 we provide a table representing the same data in supplementary materials [37].) The error associated with the determination of the number of active cells reflects a 68% confidence level. If this assay is related to single photon absorption, then biological activity might reflect the absorption spectrum of the molecule causing the photochemical effect. Within the error, the spectrum of Fig. 4(a) does not resemble the absorption spectrum of free water absorption [38], or *E. coli* in M9 media [21,39]. Moreover, the observed spectrum is at variance with prior work [21]—we found the least damage at $\lambda = 900$ nm, while Neuman and co-workers [21] found the most damage there. But Neuman *et al.* were using a different measure of viability for a different strain of *E. coli*.

To delineate links between photodamage, absorption, and viability, we tested cells that were induced *prior* to trapping. The complex photophysics of GFP gives rise to a broad one-photon excitation spectrum that peaks near $\lambda = 489$ nm [40], while the two-photon excitation spectrum peaks near $\lambda = 950$ nm. So, we expect that cells induced prior to trapping produce GFP to absorb in near $\lambda = 900$ nm with a concomitant deleterious effect on cell metabolism. Using GFP-M1 *E. coli* that were already induced with 2 mM IPTG to express eGFP, we assembled 5×5 arrays using time-shared optical traps formed from a beam with a peak power ranging from 112 to 329 mW at $\lambda = 900$ nm, holding the cells in the array for only 90 s. These conditions on power, wavelength, and hold time generally promote viability in bacteria induced after trapping—typically, we find >90% active for a peak power of ~110 mW, but when induced cells are trapped the viability collapses. As illustrated in the supplementary materials, viability is less than 20% when the cells are induced prior to trapping [37]. We attribute the collapse to an increase in (two-photon) absorption associated with the fluorescent protein.

Figure 4(a) indicates that minimizing the peak power delivered to the cell by the laser beam in an optical trap preserves viability from single photon damage. A comparison of these data with that obtained for CW traps suggests that minimizing the time-averaged power is actually what is important for viability. Figure 4(b) shows the viability obtained at continuous exposure of *E. coli* cells in a 5×5 microarray of traps to approximately 5, 10, and 20 mW trapping beams in an array formed using the SLM for wavelengths in the

range $840 \leqslant \lambda \leqslant 930$ nm. (Not all of the traps were occupied by *E. coli* [37].) These powers correspond approximately to the same time-averaged powers used in Fig. 4(a). The power and wavelength dependence of the surviving bacteria score for the CW traps track the dependence of the time-shared trap with approximately the same corresponding time-averaged power. The bacterial viability in CW traps is only slightly degraded from the time-shared traps. For example, the number of active cells at 5 mW CW power for $\lambda = 900$ nm approaches (within 20%) the viability exhibited by the time-shared trap at the same time-averaged power and wavelength. The viability is adversely affected by increasing power. For the CW traps, we find that $n = 0.73 \pm 0.04$ at 840 nm; $n = 0.73 \pm 0.01$ at 870 nm; and $n = 1.6 \pm 0.1$ at 900 nm. The number of lysed cells seems to increase with increasing power at some wavelengths (consistent with electroporation), but not others.

Higher power in a CW trap beyond the range shown in Fig. 4(b) is deadly. Neuman [21] found a LD_{50}, the time necessary to reduce the tethered cell rotation rate by 50%, for an 80 mW CW trap of 520 ± 20 s. So, we tested similar conditions by maintaining a CW trap over several cells before gelling as indicated in the Methods section. We found a dearth of active cells at 80 mW even for an exposure of only 300 s—observing green fluorescence at $\lambda = 900$ nm in only one cell in the population. Moreover, we did not observe GFP fluorescence at 80 mW power with 300 s exposure at any of the other wavelengths [37].

The results presented in Fig. 4 were obtained with the exposure time held constant while varying time-averaged trap power. The dependence on dwell time shown in the inset to Fig. 5 supports the conclusion that the time-averaged power is the dominant factor affecting viability. The data in the inset were measured in a 5×5 array formed using a 140 mW time-shared beam at $\lambda = 900$ nm. With a duty cycle of 1:25, the dwell time ranges from 10 μs to 1 ms per trap with corresponding scan frequencies that range from 40 Hz to 4 kHz. The M1 bacteria used as a control for this series of experiments showed about $90 \pm 6\%$ viability. Under these conditions, the time-averaged power, which is 5.6 mW, is independent of the dwell time—it depends only on the duty cycle. These data show that the viability is practically independent of dwell time over the range, provided that the time-averaged power is unchanged.

Reducing the *E. coli* exposure to the laser beam or the intensity of the beam seems to enhance the viability. To elucidate the origin of the photodamage, we examined the variation in viability with total energy delivered to each cell: varying the time-averaged trap power between 1.5 and 80 mW *and* the hold time in the trap between 2 and 8 min at $\lambda = 900$ nm. As illustrated in Fig. 5, the viability associated with both CW and time-shared optical traps is a monotonically decreasing function of the energy, scaling approximately linearly from 1 to 10 J according to the relation $V = -11.1E + 106$, where V denotes the percent viability and E is the energy in J. The lethal dose required to reduce viability to 50% of the population is about 5 J. This value is smaller than estimates we obtained from prior work, which typically range >20 J [21,22]. But these estimates rely on different (and presumably less sensitive) measures of viability (proton
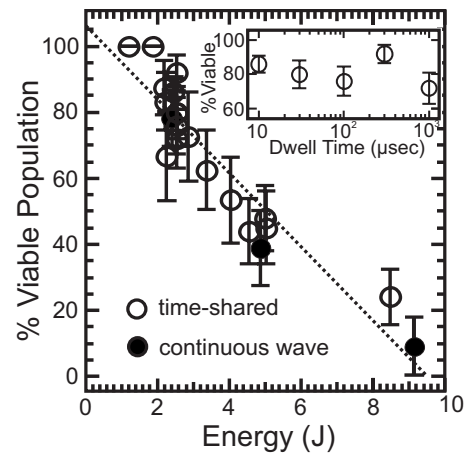

FIG. 5. Viability depends on energy. The percentage of the population that is viable (i.e., expressing GFP) after trapping is shown as a function of total energy delivered to each cell. The CW and time-shared data follow the same trend. The energy seems to be a good predictor of viability. The line fit to the data represented by the dotted line is a given by $\%V = -11.1E + 106$. An energy of about 5 J is the lethal dose associated with 50% of the community. The inset shows viability as a function of the dwell time for time-shared optical traps. 5×5 2D arrays of *E. coli* bacteria incorporating the plasmid GFP-M1 are assembled using time-shared optical traps at $\lambda = 900$ nm with a power of 140 mW in the beam. In each case the cells in the microarray are held for about 8 min prior to gelling. The percentage of the population that is viable (i.e., expressing GFP) after trapping is shown as a function of dwell time for a 1:25 duty cycle scan. Since the duty cycle is the same, the time-averaged power is independent of the dwell time. Likewise, the viability is relatively independent of dwell time.

pumping and membrane integrity). [For such high exposure (i.e., >40 J), it has been suggested that laser-irradiated eukaryotes show photothermal response [24].]

Energy or energy density has been used as a predictor of viability before, e.g., for ultrasound [41,42]. And it has been observed that there is a critical radiant exposure that facilitates the optoinjection of macromolecules like plasmid DNA into cells, beyond which viability is compromised [41]. But this threshold is usually associated with a transiently permeabilized cell membrane, resulting from a tightly focused laser beam. However, our data do not indicate that the cell membrane is generally compromised at high energy. Our data are consistent with single photon absorption as the underlying mechanism, but it seems unlikely that heating is the cause. In addition, resonant two-photon absorption by GFP filling the cells prior to trapping adversely affects viability.

A specific photochemical cause of photodamage eludes us—the spectrum is not consistent with water or *E. coli* or the media [21]. The viability does seem to be predicated on the energy delivered to the cell. Thus trapping parameters including the total exposure, peak power, duty cycle, wavelength, etc. can all be optimized for a particular application using the energy as a single predictor. For example, trapping in a flow requires a deeper trap. Accordingly, to extend the trapping time in the flow, instead of using a CW trap, the trap can be time-shared to extend the exposure while still maintaining viability.

SUMMARY

We have established the optical trapping conditions in the near IR required for preserving viability of *E. coli* measured by the gene expression of green fluorescent protein. Like CW traps, the photodamage in a time-shared trap only depends weakly on wavelength, but depends approximately linearly on peak power, which implies an effect induced by single photon absorption. Generally, for the same duration exposure, the photodamage is related to the time-averaged power, not the peak power, while for the same time-averaged power, the photodamage increases linearly with exposure.

Taken altogether, i.e., integrating the exposure time and power, the data indicate that there is a 50% lethal *energy* dose of about 5 J for *E. coli*. Thus a single parameter—the energy—is a predictor of cell viability.

[1] D. G. Grier, Nature (London) **424**, 810 (2003).

[2] A. Ashkin, Biophys. J. **61**, 569 (1992).

[3] A. Ashkin and J. M. Dziedzic, Appl. Phys. Lett. **19**, 283 (1971).

[4] A. Ashkin and J. M. Dziedzic, Science **235**, 1517 (1987).

[5] A. Ashkin, J. M. Dziedzic, and T. Yamane, Nature (London) **330**, 769 (1987).

[6] A. Ashkin, K. Schutze, J. M. Dziedzic, U. Euteneuer, and M. Schliwa, Nature (London) **348**, 346 (1990).

[7] G. M. Akselrod, W. Timp, U. Mirsaidov, Q. Zhao, C. Li, R. Timp, K. Timp, P. Matsudaira, and G. Timp, Biophys. J. **91**, 3465 (2006).

[8] F. Arai, K. Yoshikawa, T. Sakami, and T. Fukuda, Appl. Phys. Lett. **85**, 4301 (2004).

[9] J. E. Curtis, B. A. Koss, and D. G. Grier, Opt. Commun. **207**, 169 (2002).

[10] P. Jordan, H. Clare, L. Flendrig, J. Leach, J. Cooper, and M. Padgett, J. Mod. Opt. **51**, 627 (2004).

[11] P. Jordan *et al.*, Lab Chip **5**, 1224 (2005).

[12] J. E. Molloy, Methods Cell Biol. **55**, 205 (1998).

[13] M. Polin, K. Ladavac, S. H. Lee, Y. Roichman, and D. G. Grier, Opt. Express **13**, 5831 (2005).

[14] K. Visscher, S. P. Gross, and S. M. Block, IEEE J. Sel. Top. Quantum Electron. **2**, 1066 (1996).

[15] Y. Liu, G. J. Sonek, M. W. Berns, and B. J. Tromberg, Biophys. J. **71**, 2158 (1996).

[16] M. W. Berns, Biophys. J. **16**, 973 (1976).

[17] P. P. Calmettes and M. W. Berns, Proc. Natl. Acad. Sci. U.S.A. **80**, 7197 (1983).

[18] K. Konig, H. Liang, M. W. Berns, and B. J. Tromberg, Opt. Lett. **21**, 1090 (1996).

[19] K. Konig, H. Liang, M. W. Berns, and B. J. Tromberg, Nature (London) **377**, 20 (1995).

[20] K. Konig, Y. Tadir, P. Patrizio, M. W. Berns, and B. J. Tromberg, Hum. Reprod. **11**, 2162 (1996).

[21] K. C. Neuman, E. H. Chadd, G. F. Liou, K. Bergman, and S. M. Block, Biophys. J. **77**, 2856 (1999).

[22] M. B. Rasmussen, L. B. Oddershede, and H. Siegumfeldt, Appl. Environ. Microbiol. **74**, 2441 (2008).

[23] M. Ericsson, D. Hanstorp, P. Hagberg, J. Enger, and T. Nystrom, J. Bacteriol. **182**, 5551 (2000).

[24] G. Leitz, E. Fallman, S. Tuck, and O. Axner, Biophys. J. **82**, 2224 (2002).

[25] J. Bjerketorp, S. Hakansson, S. Belkin, and J. K. Jansson, Curr. Opin. Biotechnol. **17**, 43 (2006).

[26] J. Heo, K. J. Thomas, G. H. Seong, and R. M. Crooks, Anal. Chem. **75**, 22 (2003).

[27] S. J. Bryant, C. R. Nuttelman, and K. S. Anseth, J. Biomater. Sci., Polym. Ed. **11**, 439 (2000).

[28] V. A. Soifer, V. Kotlyar, and L. Doskolovich, *Iterative Methods for Diffractive Optical Elements Computation* (Taylor & Francis, London, 1997).

[29] E. Fallman and O. Axner, Appl. Opt. **36**, 2107 (1997).

[30] Carl Zeiss Objective Transmission Technical Notes.

[31] D. R. Albrecht, G. H. Underhill, A. Mendelson, and S. N. Bhatia, Lab Chip **7**, 702 (2007).

[32] D. R. Albrecht, G. H. Underhill, T. B. Wassermann, R. L. Sah, and S. N. Bhatia, Nat. Methods **3**, 369 (2006).

[33] G. M. Cruise, D. S. Scharp, and J. A. Hubbell, Biomaterials **19**, 1287 (1998).

[34] K. T. Nguyen and J. L. West, Biomaterials **23**, 4307 (2002).

[35] K. Konig, U. Simon, and K. J. Halbhuber, Cell. Mol. Biol. (Paris) **42**, 1181 (1996).

[36] R. C. Gonzalez, R. E. Woods, and S. L. Eddins, *Digital Image Processing Using MATLAB* (Pearson Prentice Hall, Upper Saddle River, NJ, 2004).

[37] See EPAPS Document No. E-PLEEE8-78-020808 for Table S1, a tabulation of the status of the cells used to generate Fig. 4; for Fig. S1, a graph of IR damage sensitivity for time-shared and CW traps with different wavelengths; for Fig. S2, a bar graph representing the population of the cells with lysed membrane, inactive, or expressive GFP that have been trapped with an 80 mW CW trap for 300 s; for Fig. S3, a bar graph illustrating the viable population of bacteria already expressing GFP trapped for 90 s. For more information on EPAPS, see http://www.aip.org/pubservs/epaps.html

[38] K. F. Palmer and D. Williams, J. Opt. Soc. Am. **64**, 1107 (1974).

[39] A. V. Belikov, G. B. Altshuler, B. T. Moroz, and I. V. Pavlovskaya, Proc. SPIE **2922**, 113 (1996).

[40] E. Spiess *et al.*, J. Microsc. **217**, 200 (2005).

[41] I. B. Clark, E. G. Hanania, J. Stevens, M. Gallina, A. Fieck, R. Brandes, B. O. Palsson, and M. R. Koller, J. Biomed. Opt. **11**, 014034 (2006).

[42] K. Keyhani, H. R. Guzmán, A. Parsons, T. N. Lewis, and M. R. Prausnitz, Pharm. Res. **18**, 1514 (2001).